JOURNAL OF MATERIALS SCIENCE 24 (1989) 2628–2636

Correlation between the structural and electrical transport properties of SnO_2 films

CHITRA AGASHE, M. G. TAKWALE, B. R. MARATHE, V. G. BHIDE
School of Energy Studies, University of Poona, Pune 411 007, India

Transparent and conducting thin films of tin oxide have been deposited by spray pyrolysis on Corning 7059 substrates. The films were investigated by X-ray diffraction and Seebeck measurements to study the structural and electrical transport properties. The films were polycrystalline and the oxide phase observed was SnO_2 in cassiterite structure. The films were preferentially oriented along [2 0 0]. Trap densities along [3 1 0] and [1 0 1] have been calculated for the first time. Assigning the traps mainly to the grain boundaries, the grain-boundary barrier height was calculated and compared with that obtained from the Seebeck measurements. A good agreement between these values was observed. The agreement was the best for films deposited under optimum deposition conditions.

1. Introduction

It has been well established that metal oxides in thin film form are preferable as transparent conducting coatings against the thin metal films. Various metal oxides have been investigated by several workers and SnO_2 has been proved to be the most stable compound. Since 1937 it has been investigated by several workers [1] and the literature shows a dependence of film properties on the process parameters.

Our previous work [2] explains the dependence of electrical properties on the structure of the films through a "texture coefficient" parameter, which describes the preferred orientation of the films. The results quoted were related mostly to the fluorine-doped SnO_2 films. The effect of substrate temperature on the film properties has also been investigated [3] from which it is clear that the structural and electrical properties at room temperature are related.

Here we report the transport properties of undoped SnO_2 films determined by Seebeck measurements over the temperature range 100 to 350 K and an attempt has been made to correlate the results to the structural properties.

2. Experimental details

The undoped SnO_2 films were spray deposited under an optimum air flow rate of 7 litre min^{-1}. The details of the experimental apparatus are given elsewhere [2]. Two sets of films have been studied. Group A consists of films deposited with different substrate temperature (with constant film thickness $\sim 0.165\,\mu m$) and group B refers to the films with variation of thickness (with constant substrate temperature $\sim 425°$ C). The range of substrate temperature was 375 to 500° C and that of film thickness was 0.08 to 0.41 μm.

The structural properties of these films were investigated by X-ray diffraction technique using both Fe$K\alpha$ ($\lambda = 0.1937$ nm) and Cu$K\alpha$ ($\lambda = 0.1542$ nm) radiations with a Philips PW 1840 diffractometer. Other conditions were kept constant while taking the diffractograms.

The electrical transport parameters were determined by Seebeck measurements. The Seebeck coefficient is used to calculate the charge carrier concentration. The electrical resistivity and thermo e.m.f. measurements over the temperature range 100 to 350 K give the variation with temperature of electrical conductivity, carrier concentration and hence the carrier mobility. The mobility data are analysed for different scattering mechanisms assuming their contributions to be independent. To establish the correlation between the electrical and structural properties, trap densities along various crystal orientations are calculated. Belanger *et al.* [4] have calculated the trap densities for [1 1 0], [3 0 1] and [2 1 1] for SnO_2. However, the calculations for [1 0 1] and [3 1 0] directions have been carried out for the first time in the present investigation.

3. Results and discussion

The undoped SnO_2 is electrically conducting mainly as a result of deviation from stoichiometry. The structure and stoichiometry of the films are determined by the process parameters: namely substrate temperature and film thickness. In the present case, film thickness was varied by varying the amount of solution sprayed, hence two independent factors seem to be involved [5]: (1) effect of time on deposition – changes in source composition and influence of substrate; (2) effect of film thickness – surface or growth-related effects. Because it was observed that the properties of films deposited from a source after repeated depositions did not vary, the composition of the source can be assumed to be unchanged. The influence of morphology of the substrate surface would be the same in the case of thin and thick films because for the same deposition conditions the incubation time is the same. Hence the time up to which the substrate surface defines the film growth is the same for thin and thick

0022–2461/89 $03.00 + .12

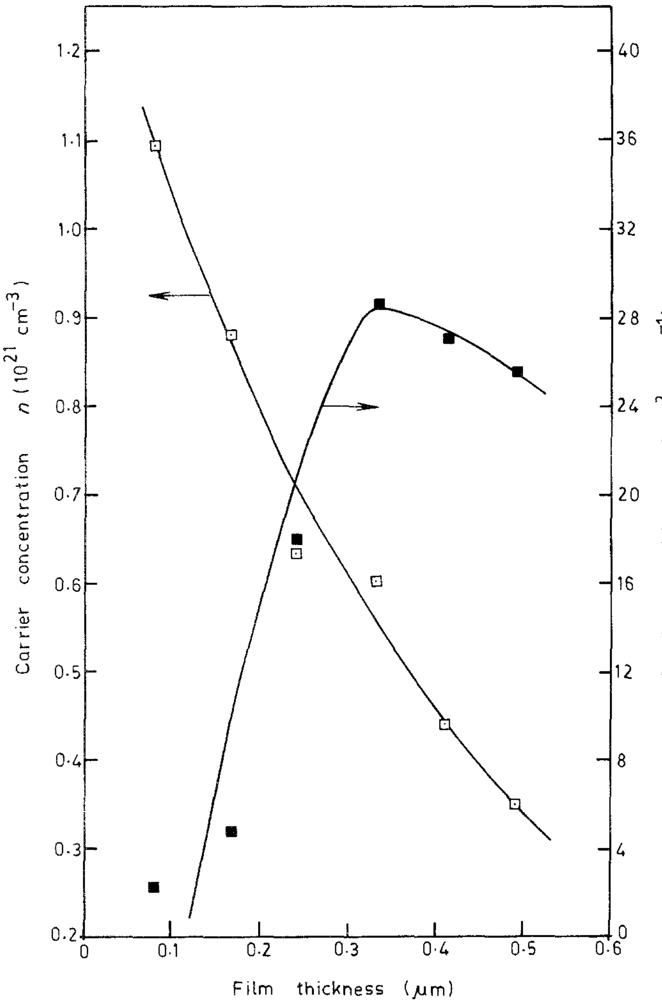

Figure 1 Variation of electrical transport parameters with film thickness.

films. Beyond this time, when the growth is further continued to make a thick film, the already grown lower layers of the film are expected to affect the structure and composition of the growing layers through an interaction between the two. The structure of the lower layers constrains the arrangement of incoming atoms and the interaction processes between them determine the composition of the growing layer. Hence as far as the growth of films is concerned the influence of substrate is the same in thin and thick films but while evaluating the film properties the effect of substrate is more in thin films and less in thick films.

In case of thin films, the effect of surface scattering is obviously more and hence we expect the film properties to improve with film thickness. Fig. 1 shows the variation of electrical transport parameters with film thickness. The mobility of charge carriers has increased with film thickness (up to $0.33\,\mu$m), but

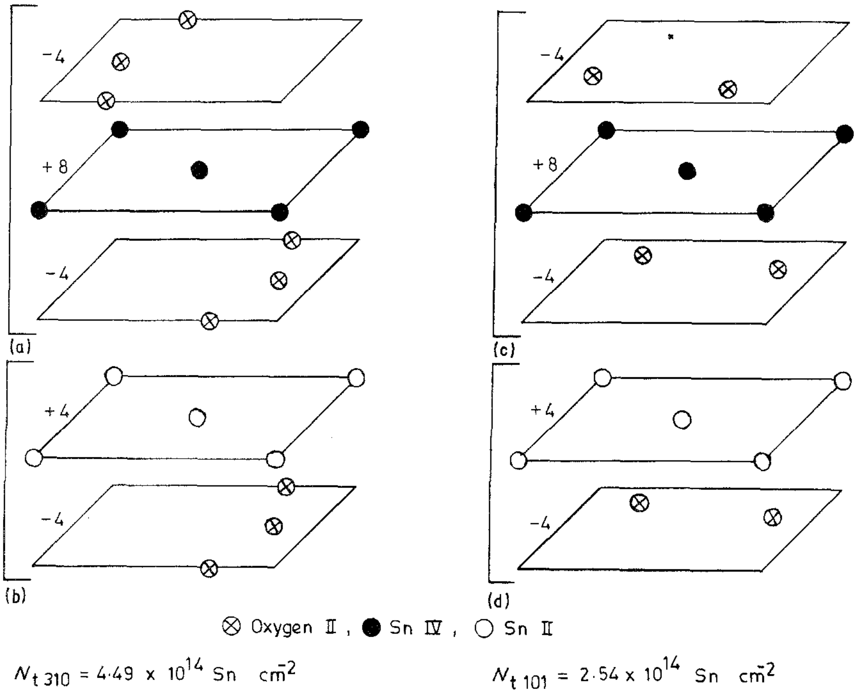

Figure 2 Crystallite surface of undoped SnO_2 having, (a) the (3 1 0) plane with an oxygen layer, (b) the (3 1 0) plane after reduction, (c) the (1 0 1) plane with an oxygen layer and (d) the (1 0 1) plane after reduction.

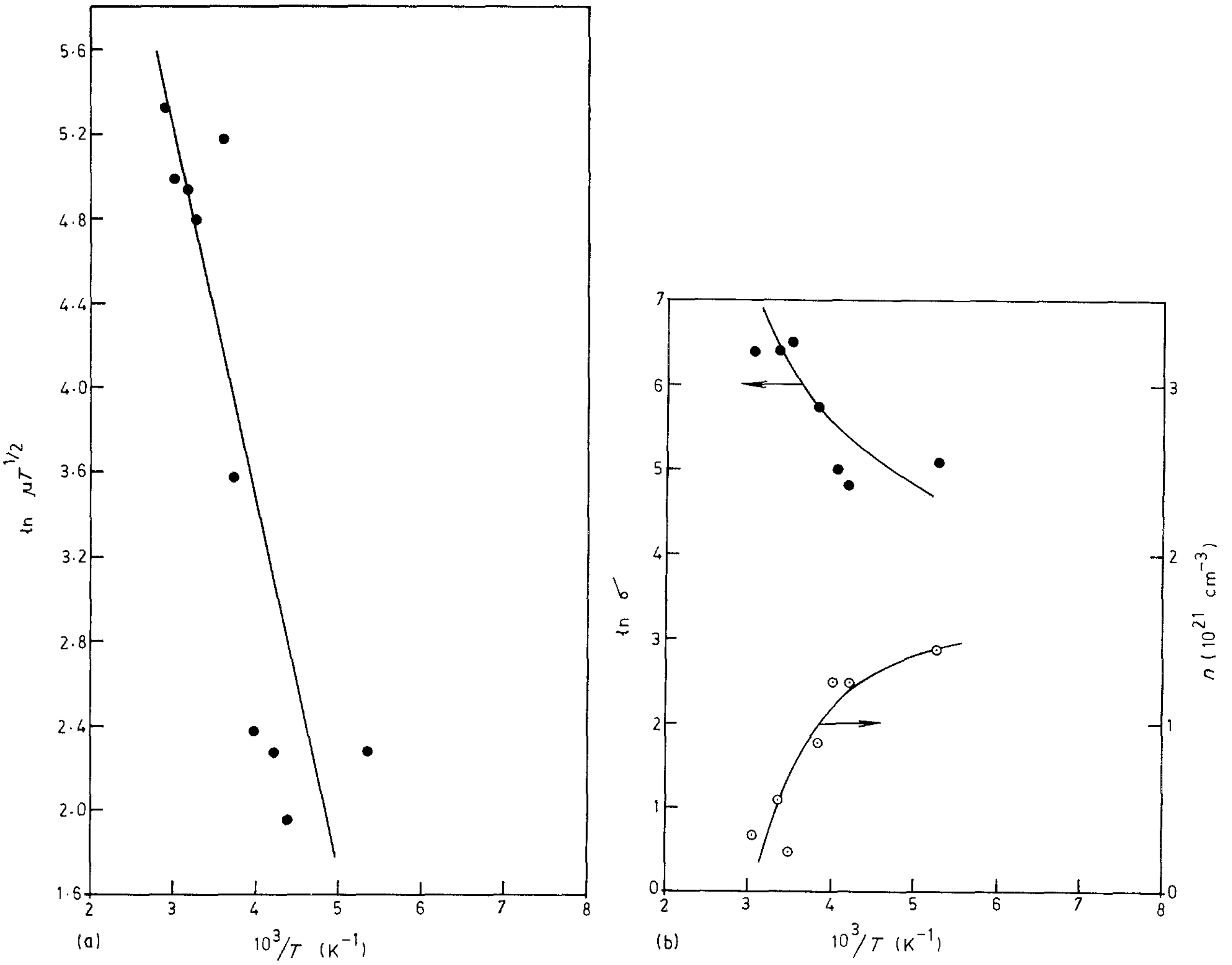

Figure 3 (a) Variation of $\ln \mu T^{1/2}$ with inverse temperature (substrate temperature 375° C, film thickness = 0.165 μm, ϕ_B = 153.24 meV. (b) Variation of carrier concentration and electrical conductivity with inverse temperature (substrate temperature 375° C).

the charge carrier concentration has decreased. Hence the film properties seem to be governed not only by surface-related phenomena, as suggested by the increase of charge carrier mobility with film thickness due to reduced surface scattering in thick films, but also by the growth mechanism (decrease of charge carrier concentration with film thickness and decrease of charge carrier mobility at higher thicknesses). The influence of growth mechanism on the charge carrier concentration could be seen as follows. During the deposition of SnO_2 films, as the layer grows, oxygen probably escapes in the atmosphere and this oxygen-deficient layer is conducting. This should repeat for subsequent layers. However, if the oxygen in the upper growing film can penetrate to the layers below, the oxygen content in the lower layers increases. This would result in an improvement in the stoichiometry of these films and hence a reduction in carrier concentration. Another possibility of higher carrier concentration in thin films could be due to a lower sticking coefficient of oxygen on the glass substrate (Corning 7059) compared to that on a grown SnO_2

TABLE I Comparison of the film properties determined from X-ray diffraction studies and Seebeck measurements

Group of films	Process parameter varied	Trap density N_t (10^{14} cm^{-2})	Grain-boundary barrier height (meV) calculated from	
			Structural studies	Seebeck measurements
A	Substrate temperature (° C)			
	375	2.651	1057.00	153.24
	400	0.360	55.00	41.79
	425	0.262	13.00	15.67
	450	0.274	27.00	19.17
	475	0.417	42.70	24.28
	500	0.515	59.40	33.62
B	Film thickness (μm)			
	0.080	0.720	79.00	81.03
	0.165	0.262	13.00	15.67
	0.330	0.248	16.75	12.75
	0.410	0.554	117.30	23.51

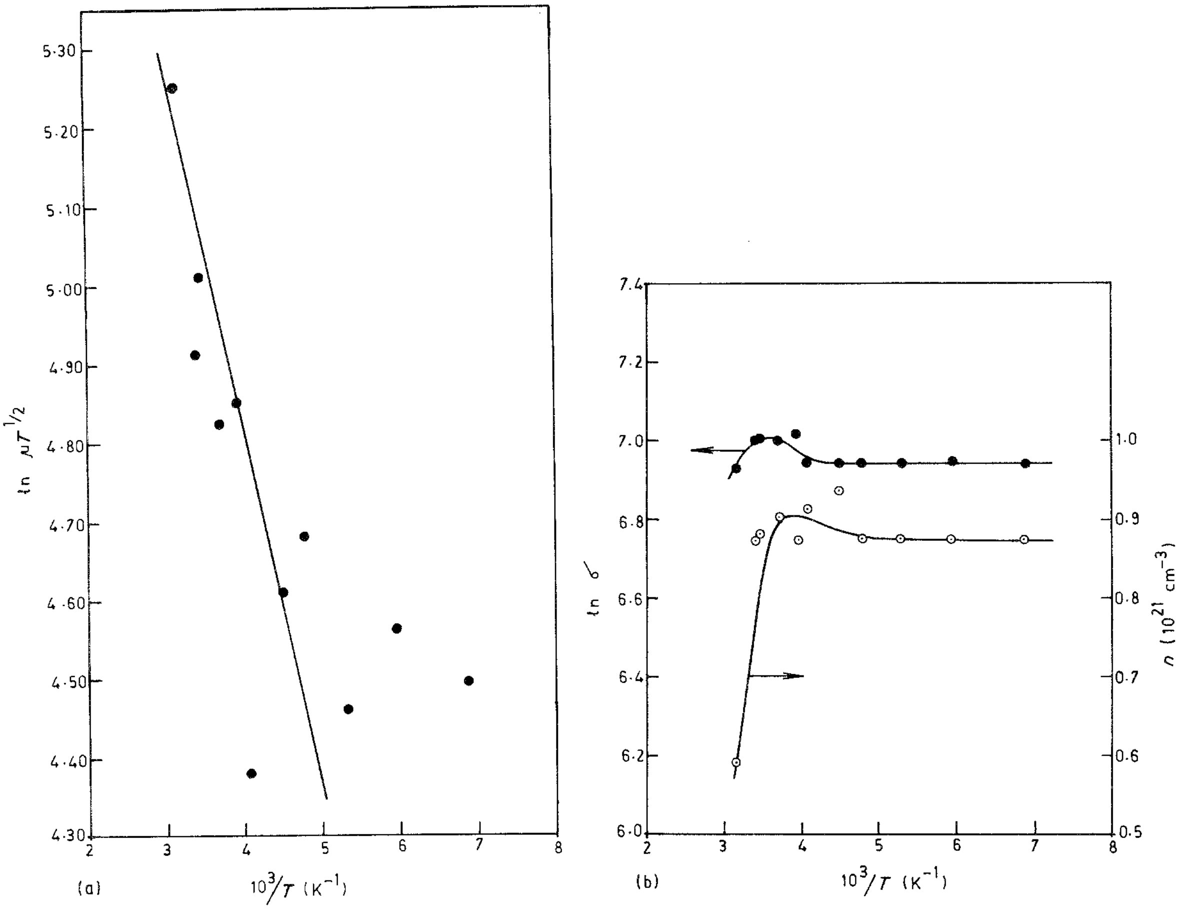

Figure 4 (a) Variation of $\ln \mu T^{1/2}$ with inverse temperature (substrate temperature 400° C, film thickness = $0.165\,\mu$m, $\phi_B = 41.79$ meV). (b) Variation of carrier concentration and electrical conductivity with inverse temperature (substrate temperature 400° C).

film, which would result in higher non-stoichiometry in thin films.

Grain boundaries are known to locate defects, impurities and more traps than within a grain. As the orientation of the grain changes, the density of traps also changes. Belanger *et al.* [4] have calculated the density of traps for different orientations, i.e. [1 1 0], [2 1 1] and [3 0 1]. Because our investigations have additional orientations ([1 0 1] and [3 1 0]), it was a good exercise to find the density of traps for these orientations, if any. Fig. 2 shows the sequence of charged planes for (1 0 1) and (3 1 0). In the highly conducting, non-stoichiometric SnO_2 films, the removal of oxygen from the upper or bottom layer of these sequences terminates the layer containing Sn^{4+} states into the layer containing Sn^{2+} states in order to follow the charge neutrality condition. These Sn^{2+} states act as electron traps. Hence for undoped SnO_2, traps are present along [1 1 0], [2 1 1], [3 0 1] [4] and [1 0 1] and [3 1 0]. The [2 0 0] and [4 0 0] orientations do not have traps [4]. Considering these points, the trap density (per unit area) was calculated from the X-ray diffraction pattern for each case. Each plane was assigned a weightage depending on its intensity in the X-ray diffraction pattern. Because the traps are assigned to the grain boundaries, the grain-boundary barrier height, θ_B, was calculated from this trap density using the relationship [6]

$$\theta_B = q^2 N_t^2 / 8\varepsilon N (\mathrm{eV}) \qquad (1)$$

where N_t is the trap density per unit area at the interface between the grains (grain boundaries) and ε is the relative permittivity of SnO_2. N is the charge carrier concentration. The results of these calculations are given in Table I.

The carrier transport mechanism was studied using the results of the Seebeck measurements. Before analysing these results a few things are discussed here for ready reference. In the non-stoichiometric SnO_2, the ionic character of the Sn–O bond is expected to be higher than 37.3% [7] and the ionic character of the bond will increase with the concentration of oxygen vacancies. Also, in this rutile type of structure of SnO_2, the Madelung constant is high. Hence the optical lattice scattering is expected to be considerable [7]. The acoustical lattice scattering would be negligible because the structure is centrosymmetric [8] but the neutral impurity scattering is operative at very low temperatures [9], not covered in the present investigation, hence it need not be considered. The ionized impurity scattering may be operative at temperatures lower than 100 K. The grain-boundary scattering was expected to be considerable in these polycrystalline films. The results of Seebeck measurements are given in Figs 3 to 11. Figs 3a to 11a are plotted as $\ln \mu T^{1/2}$ against inverse temperature, to isolate the effect of grain-boundary scattering. The barrier height is calculated from the slope of this straight line. The sudden rise of the curve at higher temperatures suggests the probability of optical lattice scattering. The very fact that the $\ln \mu T^{1/2}$ against $10^3/T$ curve is a straight line, suggests that the grain-boundary

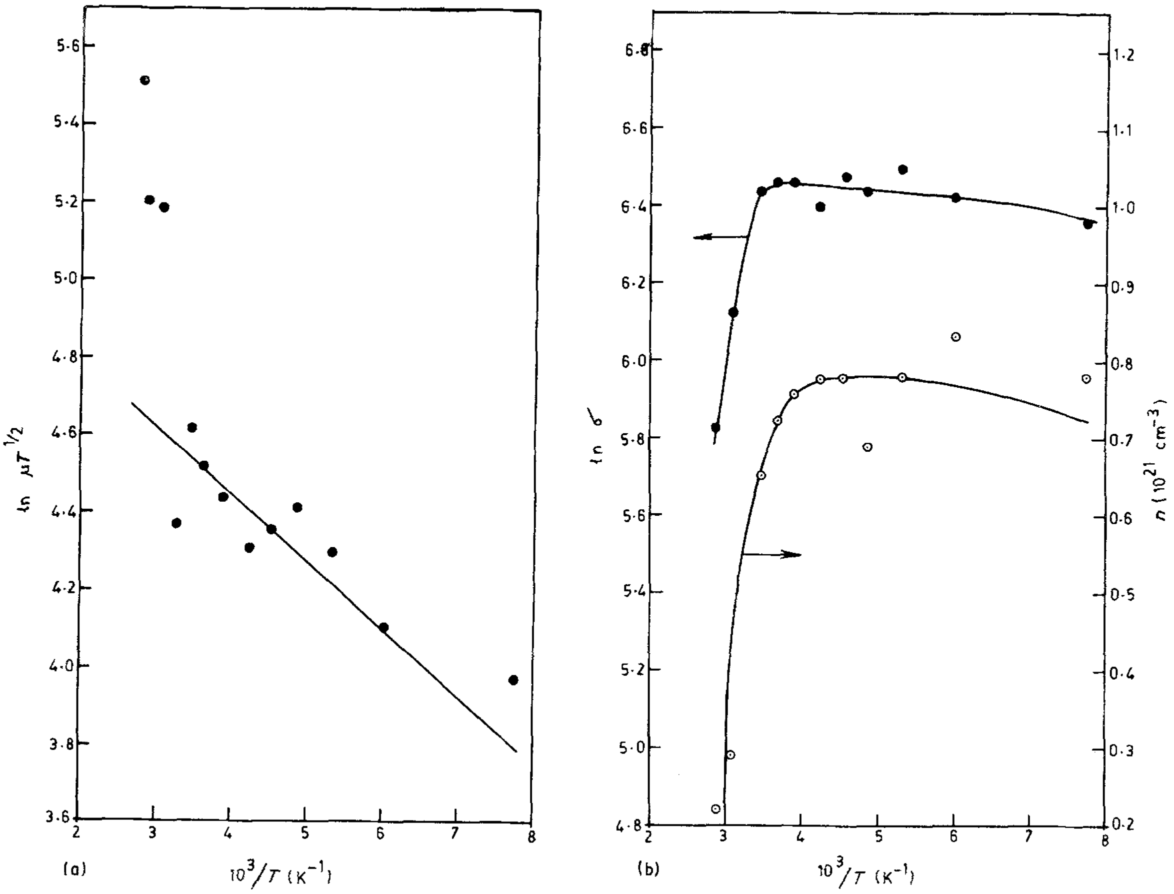

Figure 5 (a) Variation of ln $\mu T^{1/2}$ with inverse temperature (substrate temperature 425° C, film thickness = 0.165 μm, ϕ_B = 15.67 meV. (b) Variation of carrier concentration and electrical conductivity with inverse temperature (substrate temperature 425° C).

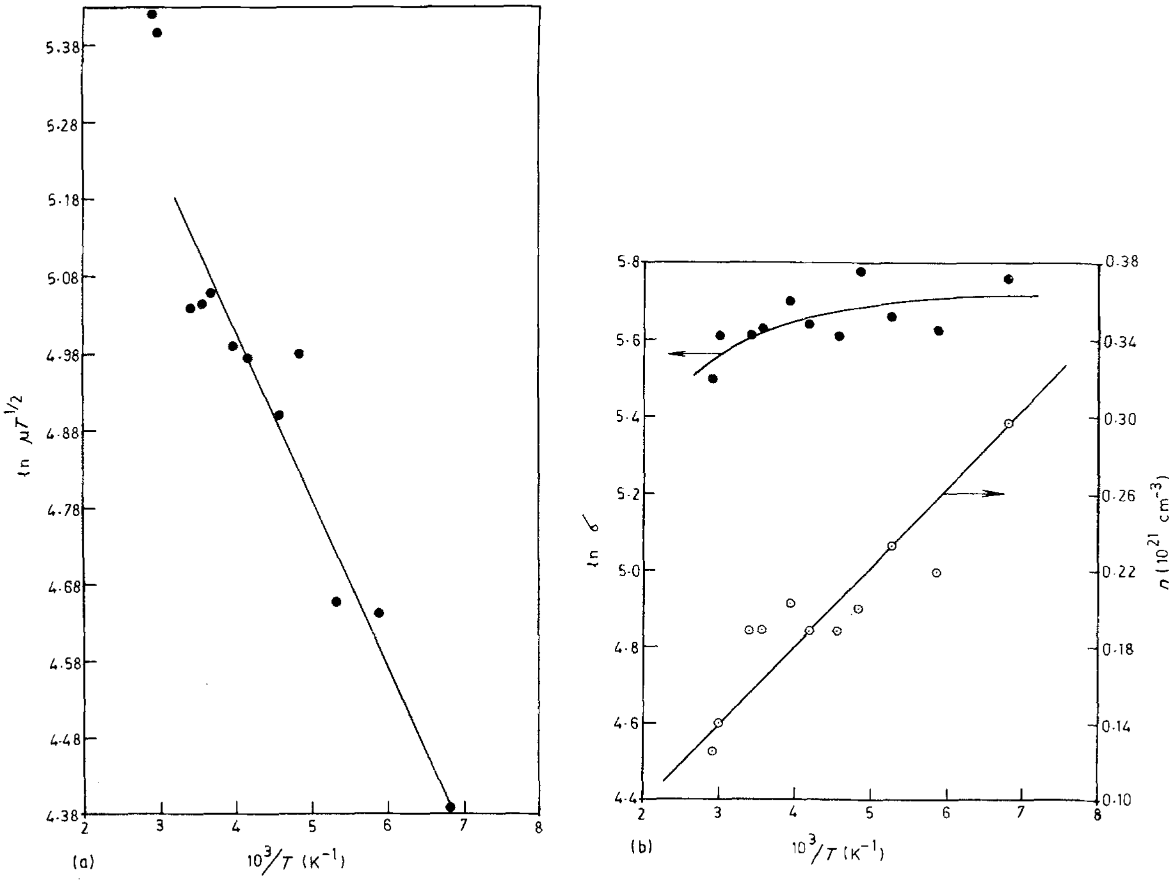

Figure 6 (a) Variation of ln $\mu T^{1/2}$ with inverse temperature (substrate temperature 450° C, film thickness = 0.165 μm, ϕ_B = 19.17 meV). (b) Variation of carrier concentration and electrical conductivity with inverse temperature (substrate temperature 450° C).

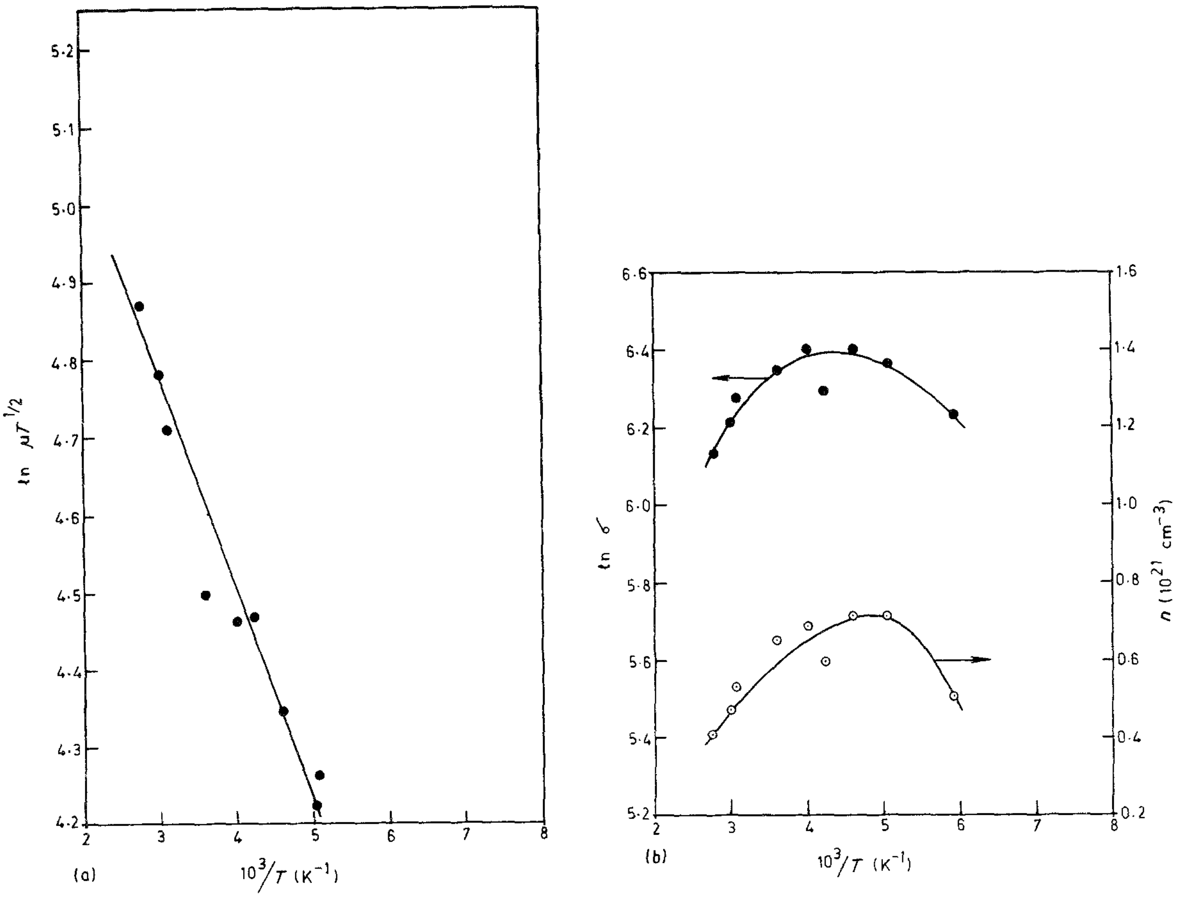

Figure 7 (a) Variation of $\ln \mu T^{1/2}$ with inverse temperature (substrate temperature 475° C, film thickness $0.165\,\mu$m, $\phi_B = 24.28$ meV). (b) Variation of carrier concentration and electrical conductivity with inverse temperature (substrate temperature 475° C).

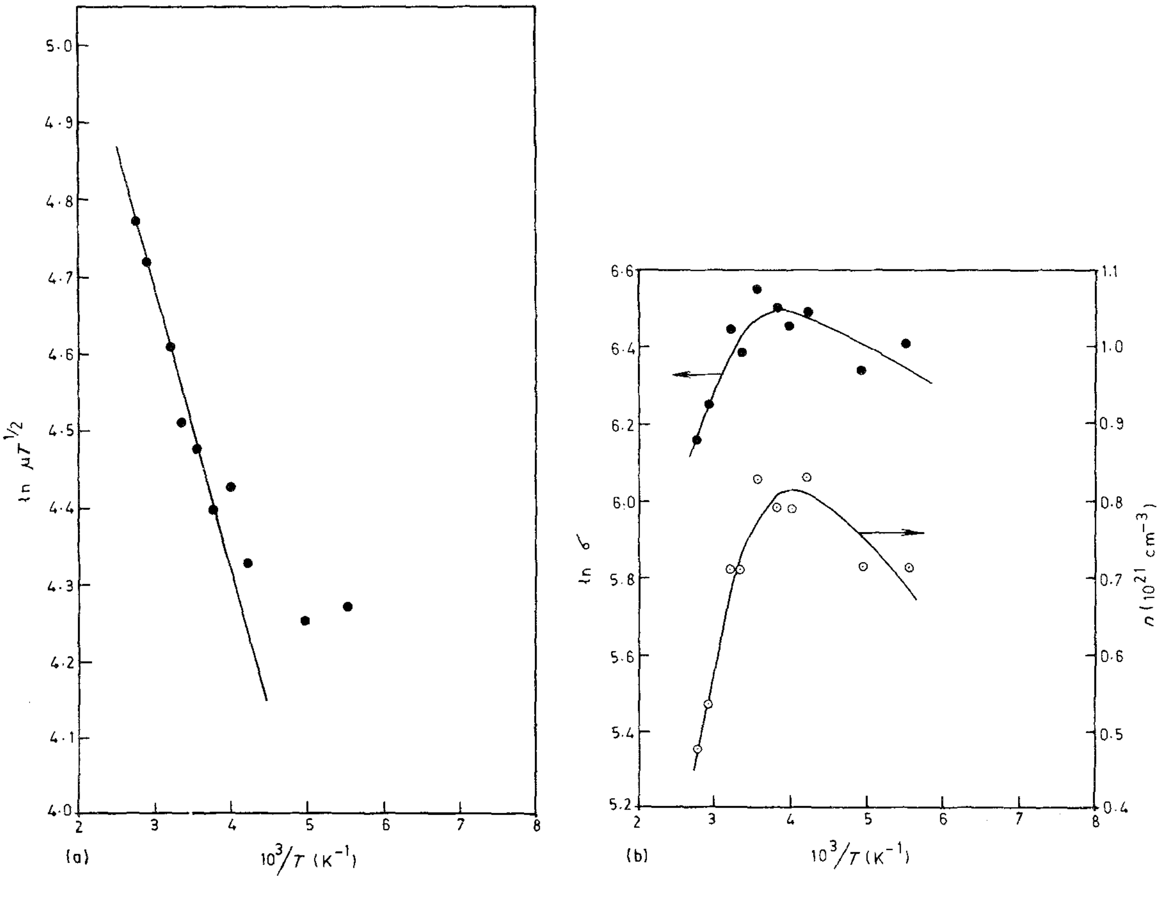

Figure 8 (a) Variation of $\ln \mu T^{1/2}$ with inverse temperature (substrate temperature 500° C, film thickness = $0.165\,\mu$m, $\phi_B = 33.62$ meV). (b) Variation of carrier concentration and electrical conductivity with inverse temperature (substrate temperature 500° C).

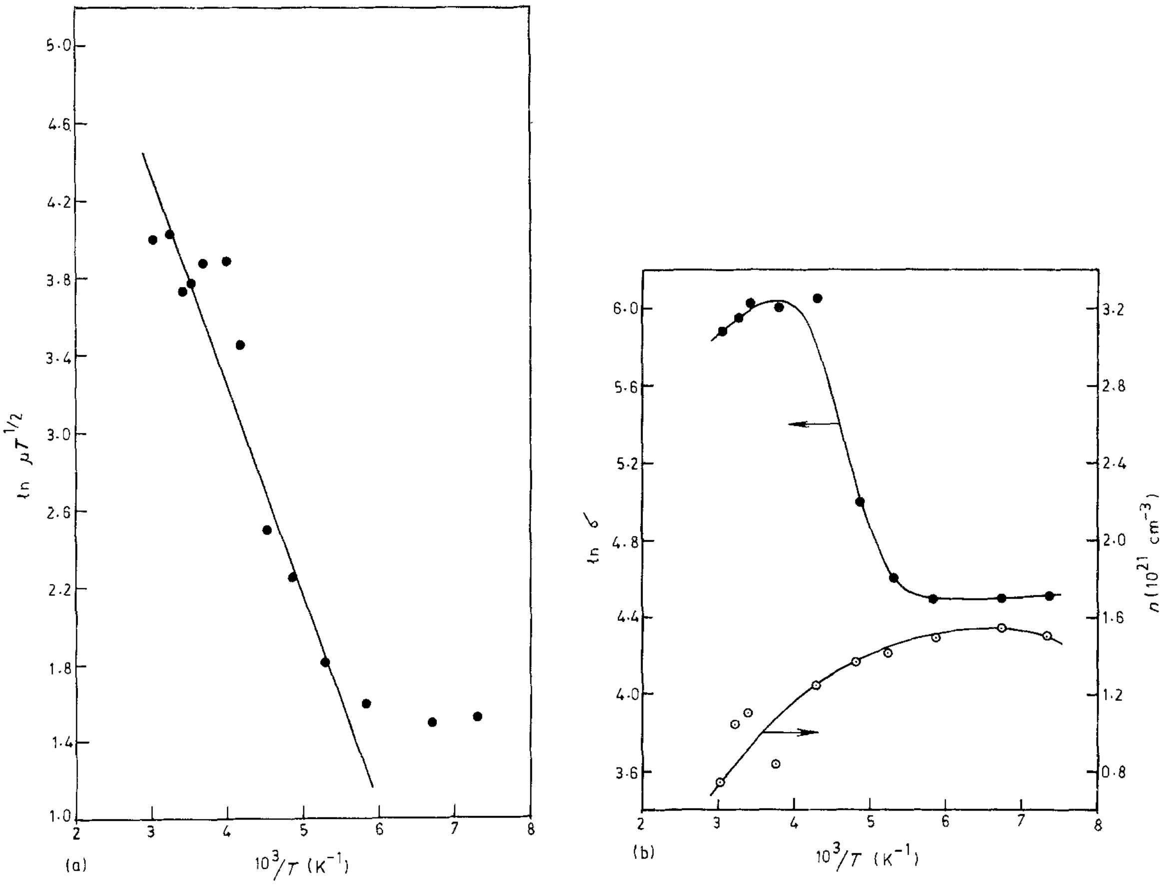

Figure 9 (a) Variation of $\ln \mu T^{1/2}$ with inverse temperature (film thickness 0.08 μm, substrate temperature = 425° C, ϕ_B = 81.03 meV). (b) Variation of carrier concentration and electrical conductivity with inverse temperature (film thickness 0.08 μm).

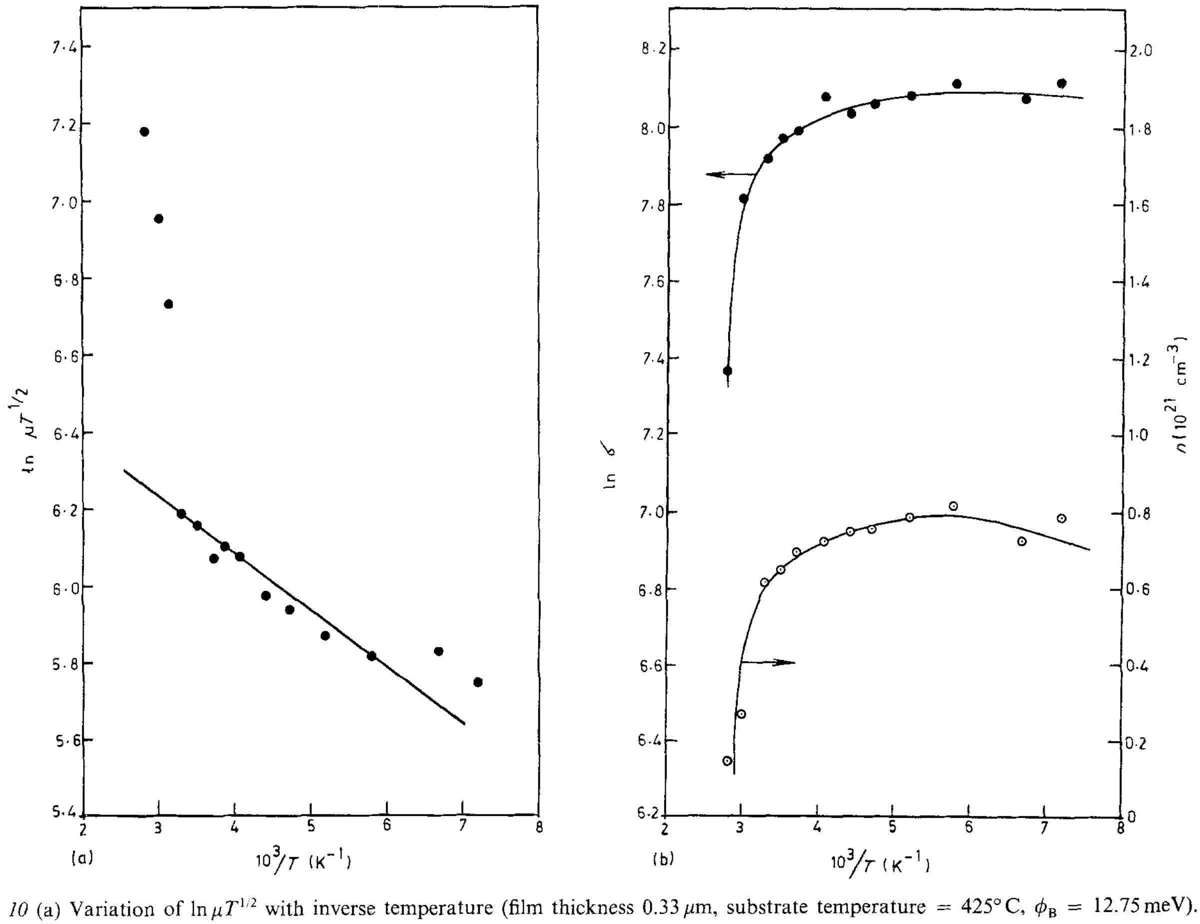

Figure 10 (a) Variation of $\ln \mu T^{1/2}$ with inverse temperature (film thickness 0.33 μm, substrate temperature = 425° C, ϕ_B = 12.75 meV). (b) Variation of carrier concentration and electrical conductivity with inverse temperature (film thickness 0.33 μm).

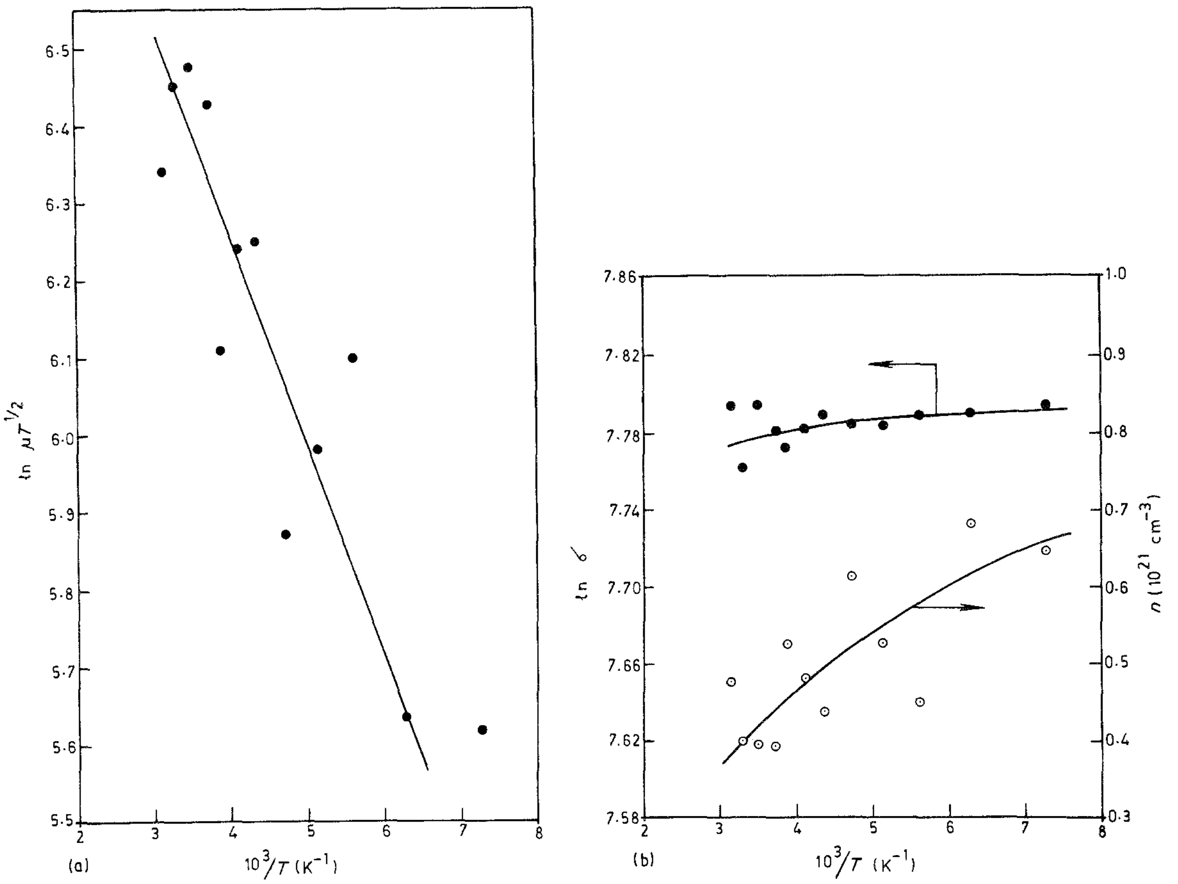

Figure 11 (a) Variation of $\ln \mu T^{1/2}$ with inverse temperature (film thickness 0.41 μm, substrate temperature = 425° C, ϕ_B = 23.51 meV). (b) Variation of carrier concentration and electrical conductivity with inverse temperature (film thickness 0.41 μm).

barrier height is constant in the temperature range studied. The grain boundary barrier height depends on the trap levels and its occupancy by the electrons. The stability of the X-ray diffraction patterns at different temperatures suggests that the trap density does not vary with temperature. Because the grain-boundary barrier height does not vary with temperature, the occupancy of traps also seems to remain constant with temperature. Additionally, the SnO_2 films are degenerate, hence, one does not expect significant changes in the carrier concentration with temperature.

In the spray pyrolysis technique, the substrate temperature is known to affect the structure and stoichiometry of the films. It has an optimum value where the film structure is better and due to the maximum deviation from stoichiometry the electrical conductivity is higher. In the present investigation, this optimum substrate temperature is 425° C.

The values of barrier height calculated from the structural details and the Seebeck measurements are given in the table and Figs 3 to 8, and show a good agreement. This agreement is the best at the optimum substrate temperature. At lower substrate temperature the structure is poor and the barrier height calculated from the structure is higher (1.057 eV). As mentioned earlier, the barrier height not only depends on the number of traps but also on their occupancy. Because the number of traps at this lower temperature is high, $2.651 \times 10^{14}\,\mathrm{cm}^{-2}$, and the majority carrier concentration is $1.113 \times 10^{21}\,\mathrm{cm}^{-3}$, not all traps are filled. This should explain the difference in grain-boundary barrier heights. If the carrier concentration had been higher than the number of traps, the high value would have been justified.

The effect of film thickness on the transport properties is also investigated (Figs 1, 5, 9, 10 and 11). The values of charge carrier concentration given in Fig. 1 are the resultant of (1) availability of charge carriers due to the deviation from stoichiometry, and (2) loss of charge carriers by trapping at the grain boundaries. The deviation from stoichiometry is a function of the gradient of oxygen concentration across the layers of the film and is determined during the growth. The loss of charge carriers is due to the trapping at the grain boundaries. As mentioned in the table, the reduced number of traps in case of films of thickness ~ 0.165 μm and higher, would have raised the value of charge carrier concentration in this range of film thickness. However, the improved stoichiometry in these films results in a lower number of charge carriers and the overall effect appears to be governed by this factor than the trapping at grain boundaries.

The variation of charge carrier mobility with film thickness is shown in Fig. 1. The charge carrier mobility increases with film thickness suggesting the presence of surface-related effects. But the reorientation and the rearrangement of the grains in case of thicker films [2] has improved the structure of the films along [200] up to film thickness of ~ 0.33 μm. During the growth of still thicker films (~ 0.41 μm) some grains are oriented along other directions which possess trap states and these increased traps in thicker films have reduced the charge carrier mobility because of higher grain-boundary barrier height. The values of grain-boundary barrier height calculated from the structural studies and the Seebeck measurements are given in Table I and Figs 5, 9, 10 and 11. A good agreement is seen in the case of films of thicknesses from ~0.165 to ~0.33 μm. It seems then that the variation of charge carrier mobility with temperature is governed mainly by the grain-boundary scattering up to 300 K. At higher temperatures the optical lattice scattering contributes to the conduction mechanism.

4. Conclusions

The films are polycrystalline. Within the detection limit of X-ray diffraction, the tin oxide phase observed was only SnO_2. The structure was tetragonal rutile (cassiterite) with preferred orientation along [2 0 0] in all cases except when deposited at 375° C. Earlier work on SnO_2 reports that the transport mechanism is contributed to by the grain boundary, ionized impurity and phonon scattering. In the present investigation the Seebeck measurements show that the grain-boundary scattering is dominant in the temperature range 100 to 300 K.

It is explained by Belanger *et al.* [4] that the [2 0 0] orientation is free of traps. Hence by calculating the trap density along [3 1 0] and [1 0 1], an attempt has been made to correlate the structural and electrical transport properties. The correlation is the best in the case of films deposited under optimum deposition conditions (substrate temperature 425° C and film thickness 0.165 μm).

Acknowledgement

This work was supported by the Council of Scientific and Industrial Research, New Delhi, India.

References

1. C. BAUER, *Ann. Phys.* **30** (1937) 433.
2. C. AGASHE, M. G. TAKWALE, B. R. MARATHE and V. G. BHIDE, *Sol. Energy Mater.* **17** (1988) 99.
3. C. AGASHE, B. R. MARATHE, M. G. TAKWALE and V. G. BHIDE, *Thin Solid Films*, **164** (1988) 261.
4. D. BELANGER, J. P. DODELET, B. A. LOMBOS and J. I. DICKSON, *J. Electrochem. Soc.* **132** (1985) 1398.
5. M. BUCHANAN, J. B. WEBB and D. F. WILLIAMS, *Thin Solid Films* **80** (1981) 373.
6. Y. S. HSU and S. K. GHANDHI, *J. Electrochem. Soc.* **127** (1980) 1595.
7. K. ISHIGURO, T. SASAKI, T. ARAI and I. IMAI, *J. Phys. Soc. Jpn* **13** (1958) 296.
8. J. A. MARLEY and R. C. DOCKERTY, *Phys. Rev.* **140** (1965) A 304.
9. G. E. STILLMAN and C. M. WOLFE, *Thin Solid Films* **31** (1976) 69.

Received 7 July
and accepted 6 October 1988